



**Providing Choice & Value**  
Generic CT and MRI Contrast Agents

**FRESENIUS  
KABI**

**CONTACT REP**

**AJNR**

**Idiopathic Intracranial Hypertension is  
Associated with a Higher Burden of Visible  
Cerebral Perivascular Spaces: The  
Glymphatic Connection**

O. Jones, J. Cutsforth-Gregory, J. Chen, M.T. Bhatti, J.  
Huston and W. Brinjikji

This information is current as  
of July 29, 2025.

*AJNR Am J Neuroradiol* 2021, 42 (12) 2160-2164  
doi: <https://doi.org/10.3174/ajnr.A7326>  
<http://www.ajnr.org/content/42/12/2160>

# Idiopathic Intracranial Hypertension is Associated with a Higher Burden of Visible Cerebral Perivascular Spaces: The Glymphatic Connection

O. Jones, J. Cutsforth-Gregory, J. Chen, M.T. Bhatti, J. Huston, and W. Brinjikji

## ABSTRACT

**BACKGROUND AND PURPOSE:** Research suggests a connection between idiopathic intracranial hypertension and the cerebral glymphatic system. We hypothesized that visible dilated perivascular spaces, possible glymphatic pathways, would be more prevalent in patients with idiopathic intracranial hypertension. This prevalence could provide a biomarker and add evidence to the glymphatic connection in the pathogenesis of idiopathic intracranial hypertension.

**MATERIALS AND METHODS:** We evaluated 36 adult (older than 21 years of age) patients with idiopathic intracranial hypertension and 19 controls, 21–69 years of age, who underwent a standardized MR imaging protocol that included high-resolution precontrast T2- and T1-weighted images. All patients had complete neuro-ophthalmic examinations for papilledema. The number of visible perivascular spaces was evaluated using a comprehensive 4-point qualitative rating scale, which graded the number of visible perivascular spaces in the centrum semiovale and basal ganglia; a 2-point scale was used for the midbrain. Readers were blinded to patient diagnoses. Continuous variables were compared using a Student *t* test.

**RESULTS:** The mean number of visible perivascular spaces overall was greater in the idiopathic intracranial hypertension group than in controls (4.5 [SD, 1.9] versus 2.9 [SD, 1.9], respectively;  $P = .004$ ). This finding was significant for centrum semiovale idiopathic intracranial hypertension (2.3 [SD, 1.4] versus controls, 1.3 [SD, 1.1],  $P = .003$ ) and basal ganglia idiopathic intracranial hypertension (1.7 [SD, 0.6] versus controls, 1.2 [SD, 0.7],  $P = .009$ ). There was no significant difference in midbrain idiopathic intracranial hypertension (0.5 [SD, 0.5] versus controls, 0.4 [SD, 0.5],  $P = .47$ ).

**CONCLUSIONS:** Idiopathic intracranial hypertension is associated with an increased number of visible intracranial perivascular spaces. This finding provides insight into the pathophysiology of idiopathic intracranial hypertension, suggesting a possible relationship between idiopathic intracranial hypertension and glymphatic dysfunction and providing another useful biomarker for the disease.

**ABBREVIATIONS:** IIH = idiopathic intracranial hypertension; PVS = perivascular spaces

Idiopathic intracranial hypertension (IIH), formerly known as pseudotumor cerebri and benign intracranial hypertension, is a disease of increased intracranial pressure without an identifiable cause.<sup>1,2</sup> Recently, a number of groups have postulated that the primary insult resulting in IIH could be dysfunction in CSF clearance via glymphatic pathways in the brain parenchyma.<sup>3–8</sup>

Briefly, the glymphatic system is a pseudolymphatic network in the brain performing a waste-clearance function via movement of CSF and interstitial fluid. Much of the glymphatic clearance is dependent on perivascular spaces (PVS). CSF is

produced by the choroid plexus and exits the ventricular system via the foramina of Magendie and Luschka to the subarachnoid space. From the subarachnoid space, it enters the periarterial spaces (ie, PVS), traveling from the cortex toward the deep white matter along the courses of pial and perforator arteries in a centripetal distribution.<sup>9</sup> From the periarterial spaces, CSF is driven into the brain interstitium via aquaporin channels, mostly formed by the footplates of astrocytes.<sup>10</sup> CSF influx drives existing interstitial fluid back into the perivenous spaces surrounding large-caliber draining veins (Fig 1).<sup>9</sup> How CSF is reabsorbed at the large-caliber veins remains unclear, but a dural lymphatic pathway and a venous outflow pathway have been proposed, using dural lymphatic channels and arachnoid granulations, respectively.<sup>4</sup>

It has been hypothesized that in IIH, there is congestion of the lymphatic CSF outflow pathway of the glymphatic system.<sup>3,4</sup>

Received March 29, 2021; accepted after revision August 22.

From the Departments of Radiology (O.J., J.H., W.B.), Neurology (J.C.-G., J.C., M.T.B.), and Ophthalmology (J.C., M.T.B.), Mayo Clinic, Rochester, Minnesota.

Please address correspondence to Waleed Brinjikji, MD, Department of Radiology, Mayo Clinic, 200 First St SW, Rochester MN 55905; e-mail: brinjikji.waleed@mayo.edu; @wbrinjikji

<http://dx.doi.org/10.3174/ajnr.A7326>

In other words, there may be impaired transport of interstitial fluid from the glymphatic system to the venous blood of the dural venous sinuses, triggering a cascade of events resulting in IIH.

A multitude of brain and orbital MR imaging findings have been associated with IIH.<sup>11</sup> The most sensitive MR imaging correlate is transverse sinus stenosis.<sup>12</sup> Other findings include the appearance of an empty sella (>50% CSF filling of the sella with pituitary displacement), flattening of the posterior globes, protrusion of the optic nerve discs, and CSF enlarged/tortuous optic nerve sheaths.<sup>11,13</sup>

One imaging finding that has not been studied in association with IIH is the presence of dilated PVS, which have been proposed to be a component of the glymphatic pathway and can be dilated in a number of disease states associated with glymphatic disease, including small-vessel disease, dementia, multiple sclerosis, and other autoimmune diseases.<sup>14–23</sup> As discussed by others, we hypothesize that there is an element of glymphatic dysfunction in IIH. Because PVS have been shown to be a part of the glymphatic clearance pathway, we hypothesize that dilated PVS visible on T2-weighted MR imaging sequences are associated with IIH. Demonstrating this connection could provide valuable evidence toward glymphatic dysfunction contributing to the pathophysiology of IIH. This may serve as both a useful imaging biomarker for the disease as well as a potential therapeutic target.

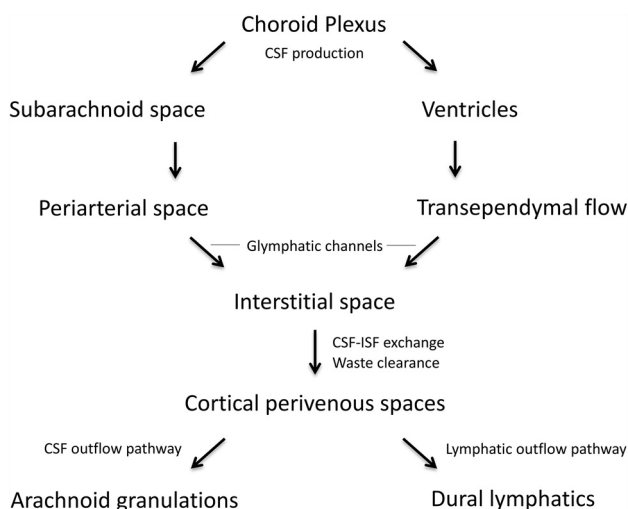


**FIG 1.** CSF-glymphatic flow chart. CSF is produced in the choroid plexus and takes a periarterial and/or a transepndymal course into the interstitial space, displacing pre-existing interstitial fluid into cortical perivenous spaces where it is absorbed by arachnoid granulations and/or dural lymphatics. ISF indicates interstitial fluid.

## MATERIALS AND METHODS

### Patient Population

Adult patients with IIH were included if they met the diagnostic criteria put forth by Friedman et al<sup>13</sup> and had ophthalmologic evidence of papilledema.

Age-matched patients (SD, 2 years) in the control group were enrolled in accordance with the following criteria: a completed MR imaging examination without a diagnosis of intracranial hypertension as established by the above-mentioned criteria and without abnormalities on MR imaging. Patients with incomplete or poor-quality MRIs were excluded.

### Imaging Protocol

The MR imaging protocol included high-resolution T2 and T1 MPRAGE precontrast images on various (GE Healthcare) 3T scanners with an 8-channel head coil. Some but not all patients underwent FLAIR imaging. Patients were scanned without sedation. The parameters for fast spin-echo T2-weighted imaging were the following: TR = 5234 ms; TE = 95.744 ms; section thickness = 4 mm without a gap; FOV = 220 mm; and matrix size = 320 × 320. All patients also underwent a 2D-TOF MR venography with TR = 29, TE = 3.3, number of excitations = 1, and matrix size = 256 × 256.

### Imaging Evaluation

Two radiologists, a neuroradiology fellow and a staff radiologist, quantified the number of PVS using a comprehensive qualitative rating scale that has been shown to have good observer agreement and was validated by Potter et al.<sup>24</sup> The radiologists rated the following sites: basal ganglia, centrum semiovale, and midbrain PVS. Basal ganglia and centrum semiovale PVS were rated 0 (none), 1 (1–10), 2 (11–20), 3 (21–40), and 4 (>40), and midbrain PVS were rated 0 (nonvisible) or 1 (visible). T2-weighted images were used to quantify the PVS. T1-weighted images and FLAIR images (if available) were used to differentiate between PVS and other lesions.

### Statistical Analysis

We calculated  $\kappa$  statistics for rating, assessed the consistency in the use of categories of PVS (Bhapkar test), and reviewed sources of discrepancy.

## RESULTS

The visible number of overall PVS was higher in patients with IIH than in the control group (IIH mean total, 4.5 [SD, 1.9] versus controls, 2.9 [SD, 1.9];  $P = .004$ ). Findings are summarized in Table 1. This was true for all sites quantified except the midbrain: IIH centrum semiovale (2.3 [SD, 1.4] versus control centrum semiovale, 1.3 [SD, 1.1],  $P = .003$ ); IIH basal ganglia (1.7 [SD, 0.6] versus control basal ganglia, 1.2 [SD, 0.7],  $P = .009$ ); and IIH midbrain (0.5

**Table 1: Quantification of perivascular spaces by site in patients with IIH versus controls**

Location	IIH Mean No. of Dilated PVS (SD)	Control Mean No. of Dilated PVS (SD)	P Value	$\kappa$ Value (mean) (range)
Centrum semiovale	2.3 (1.4)	1.3 (1.1)	.003	0.58 (0.51–0.67)
Basal ganglia	1.7 (0.6)	1.2 (0.7)	.009	0.85 (0.81–0.89)
Midbrain	0.5 (0.5)	0.4 (0.5)	.47	0.47 (0.40–0.54)
Total	4.5 (1.9)	2.9 (1.9)	.004	0.71 (0.65–0.76)

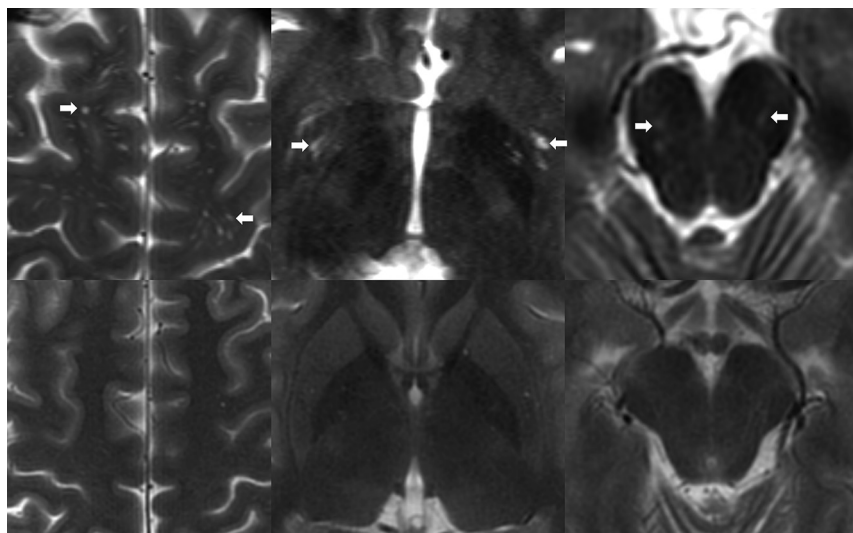


**FIG 2.** Fast spin-echo T2-weighted high-resolution images showing dilated PVS in the midbrain in a patient with IIH (upper row) and a healthy control (lower row). Elongated CSF-filled structures (arrows) are seen in the expected locations: centrum semiovale supratentorial white matter (left), basal ganglia (middle), and midbrain (right).

**Table 2: Baseline characteristics<sup>a</sup>**

	IIH	Control	P Value
No.	32	21	
Age (yr)	34.8 (9.2)	37.8 (13.5)	.38
No. (%) female sex	30 (93.8)	15 (71.4)	.03
Papilledema	32 (100.0)	0 (0.0)	<.0001
Headaches	31 (96.9)	7 (33.3)	<.0001
Pulsatile tinnitus	25 (75.0)	3 (14.3)	<.0001
Highest opening pressure	360 (133.5)	185 (35.3)	.01

<sup>a</sup>The average age between patients with IIH and healthy controls was similar. Most patients with IIH were women. More patients with IIH had papilledema, headaches, and pulsatile tinnitus. CSF opening pressure was lower in patients with IIH.

[SD, 0.5] versus control midbrain, 0.4 [SD, 0.5],  $P = .47$ ). Interobserver agreement for the measurement of PVS was good ( $\kappa = 0.71$  overall). By region, the  $\kappa$  statistic for the centrum semiovale was 0.58, for the basal ganglia, it was 0.85, and midbrain, 0.47. An example of dilated PVS in a patient with IIH and a healthy control is shown in Fig 2.

Baseline characteristics between the IIH group and healthy controls are in given Table 2. Average age was similar between the IIH group and healthy controls (IIH, 34.8 versus controls, 37.8 years;  $P = .38$ ). There were more women in the IIH group (IIH, 30, versus controls, 15;  $P = .03$ ). Papilledema, headaches, and pulsatile tinnitus were present in most of the IIH group and in a few healthy controls ( $P < .0001$ ). Average highest opening pressure was 360 cm of water in the IIH group and 185 in the control group ( $P < .01$ ). Four of 21 patients in the control group had evidence of venous sinus stenosis compared with 31 of 32 patients with IIH ( $P < .0001$ ).

## DISCUSSION

We found an increased number of dilated PVS in patients with IIH compared with controls. This correlation suggests a

pathophysiologic role of the glymphatic system in IIH. Such a connection has been hypothesized in prior work on the roles of the glymphatic system in CSF accumulation and regulation.<sup>4,9,10</sup>

The presence of dilated PVS has been correlated with other disease states and is hypothesized to represent glymphatic disease. Glymphatic function is mediated by perivascular channels lined with aquaporin-4, cerebrovascular pulsatility, and metabolic waste clearance. Mestre et al<sup>25</sup> hypothesized that impairment of these components may have implications for the pathophysiology of small-vessel diseases. Perivascular spaces and their aquaporin-4 components must be structurally and functionally sound for proper glymphatic function, as confirmed by Iliff et al,<sup>26</sup> who used in vivo 2-photon imaging of small fluorescent tracers showing

impaired glymphatic flow and function in animals lacking aquaporin-4. Impaired clearance of fluorescent-tagged amyloid  $\beta$  was also found, which may be significant for understanding Alzheimer disease. Iliff et al hypothesize that bulk perivascular CSF flow is impaired by glymphatic dysfunction due to vascular remodeling, enlarged perivascular spaces, aggregation of amyloid  $\beta$  in Alzheimer disease, and aggregation of granular osmophilic material in CADASIL. Of note, the largest observed CSF influxes, as demonstrated by fluorescent glymphatic flow imaging, are along the ventral perforating arteries of the basal ganglia, a common site for enlarged perivascular space formation.<sup>26,27</sup> Enlarged PVS are ubiquitous in almost all small-vessel diseases<sup>28-30</sup> and are independently associated with risk factors for small-vessel diseases, including hypertension and advanced age.<sup>31-33</sup>

Lenck et al<sup>4</sup> hypothesized that IIH appears to be related to glymphatic system overload. They hypothesized that overflow of the lymphatic CSF outflow pathway results in venous CSF outflow pathway restriction. In other words, if one pathway fails, the other must compensate. We speculate that impairment of interstitial fluid transport from the glymphatic system to dural venous sinus blood may trigger the hydrodynamic cascade of IIH. The degree of raised intracranial pressure may depend on the efficiency of the glymphatic system to compensate with augmented CSF reabsorption. Consequently, MR imaging signs of CSF hypertension such as transverse sinus stenosis and CSF dilated optic nerve sheaths may be a direct consequence of the overloaded glymphatic system and impaired CSF reabsorption.

Bezerra et al,<sup>3</sup> similarly, hypothesized that glymphatic dysfunction is a major contributor to the development of IIH. They hypothesized that diffuse interstitial fluid retention is a result of impaired glymphatic function from either augmented arterial perivascular space overflow into the interstitial fluid, impaired outflow of the interstitial fluid into the PVS, or both. In other words, the problem may be one of excessive inflow and/or



deficient outflow within the glymphatic pathway schematized in Fig 1. This hypothesis is supported by the fact that IIH-related vision loss is related to excessive fluid in the optic nerve sheaths, likely owing to impaired dural pathway glymphatic outflow along the glymphatics of the cranial nerves. Most interesting, patients with obesity, who have higher rates of IIH in general, are known to have a higher burden of perivascular and lymphatic dysfunction; this finding could lend further support to the glymphatic dysfunction hypothesis of IIH.

Patients with IIH have a substantially increased volume of extraventricular CSF and interstitial fluid,<sup>34</sup> including the PVS.<sup>4</sup> If glymphatic congestion increases interstitial and perivascular space fluid volume, this increase should contribute to increased intracranial pressure by the Monro-Kellie hypothesis. CSF-filled, dilated PVS may serve as a potential marker for the disease.

Our study has several limitations. First, ours is a hypothesis-generating study. Given the connection between an increased number of dilated PVS and glymphatic dysfunction demonstrated with other diseases and the growing number of groups hypothesizing that IIH is, in some respect, a glymphatic disorder, we sought to identify a biomarker that could allow testing of this hypothesis and lead to further study. Additional limitations include the small number of patients included, possible confounding in matching healthy controls for sex and body mass index, lack of automation in quantifying PVS, and a possible slight variance in imaging quality between studies due to patient and technical factors. Future studies with patients will be needed to confirm the association between an increased number of dilated PVS, glymphatic dysfunction, and IIH. An automated segmentation for quantifying dilated PVS such as that used by Potter et al<sup>24</sup> may be useful in eliminating interobserver variability. However, 2 observers were involved in this study with good interobserver variability. All patients received the same imaging protocol as it relates to quantifying the number of PVS, so variability related to technical factors was limited.

## CONCLUSIONS

IIH is associated with dilated intracranial PVS, which may be detected with high-resolution T2-weighted MR imaging. These findings could provide valuable insight into the pathophysiology of IIH as it relates to glymphatic dysfunction. Future studies are needed to clarify whether the number of perivascular spaces is a biomarker in IIH disease.

## ACKNOWLEDGMENTS

The authors thank Sonia Watson, PhD, for assistance in preparation of the manuscript.

Disclosures: Jeremy Cutsforth-Gregory—UNRELATED: Royalties: Oxford University Press, Comments: Mayo Clinical Medical Neurosciences (textbook). M. Tariq Bhatti—UNRELATED: Consultancy: Receptos.

## REFERENCES

- Markey KA, Mollan SP, Jensen RH, et al. **Understanding idiopathic intracranial hypertension: mechanisms, management, and future directions.** *Lancet Neurol* 2016;15:78–91 [CrossRef Medline](#)
- Wall M. **Idiopathic intracranial hypertension.** *Neurol Clin* 2010;28:593–617 [CrossRef Medline](#)
- Bezerra MLS, Ferreira A, de Oliveira-Souza R. **Pseudotumor cerebri and glymphatic dysfunction.** *Front Neurol* 2017;8:734 [CrossRef Medline](#)
- Lenck S, Radovanovic I, Nicholson P, et al. **Idiopathic intracranial hypertension: the veno glymphatic connections.** *Neurology* 2018;91:515–22 [CrossRef Medline](#)
- Mangalore S, Rakshith S, Srinivasa R. **Solving the riddle of “idiopathic” in idiopathic intracranial hypertension and normal pressure hydrocephalus: an imaging study of the possible mechanisms—Monro-Kellie 3.0.** *Asian J Neurosurg* 2019;14:440–52 [CrossRef Medline](#)
- Mollan SP, Ali F, Hassan-Smith G, et al. **Evolving evidence in adult idiopathic intracranial hypertension: pathophysiology and management.** *J Neurol Neurosurg Psychiatry* 2016;87:982–92 [CrossRef Medline](#)
- Mondejar V, Patsalides A. **The role of arachnoid granulations and the glymphatic system in the pathophysiology of idiopathic intracranial hypertension.** *Curr Neurol Neurosci Rep* 2020;20:20 [CrossRef Medline](#)
- Nicholson P, Kedra A, Shotar E, et al. **Idiopathic intracranial hypertension: glymphedema of the brain.** *J Neuroophthalmol* 2021;41:93–97 [CrossRef Medline](#)
- Benveniste H, Lee H, Volkow ND. **The glymphatic pathway: waste removal from the CNS via cerebrospinal fluid transport.** *Neuroscientist* 2017;23:454–65 [CrossRef Medline](#)
- Jessen NA, Munk AS, Lundgaard I, et al. **The glymphatic system: a beginner's guide.** *Neurochem Res* 2015;40:2583–99 [CrossRef Medline](#)
- Rehder D. **Idiopathic intracranial hypertension: review of clinical syndrome, imaging findings, and treatment.** *Curr Probl Diagn Radiology* 2020;49:205–14 [CrossRef Medline](#)
- Morris PP, Black DF, Port J, et al. **Transverse sinus stenosis is the most sensitive MR imaging correlate of idiopathic intracranial hypertension.** *AJNR Am J Neuroradiol* 2017;38:471–77 [CrossRef Medline](#)
- Friedman DI, Liu GT, Digre KB. **Revised diagnostic criteria for the pseudotumor cerebri syndrome in adults and children.** *Neurology* 2013;81:1159–65 [CrossRef Medline](#)
- Boespflug EL, Simon MJ, Leonard E, et al. **Targeted assessment of enlargement of the perivascular space in Alzheimer's disease and vascular dementia subtypes implicates astroglial involvement specific to Alzheimer's disease.** *J Alzheimers Dis* 2018;66:1587–97 [CrossRef Medline](#)
- Chabriet H, Joutel A, Dichgans M, et al. **CADASIL.** *Lancet Neurol* 2009;8:643–53 [CrossRef Medline](#)
- Cordonnier C, Al-Shahi Salman R, Wardlaw J. **Spontaneous brain microbleeds: systematic review, subgroup analyses and standards for study design and reporting.** *Brain* 2007;130:1988–2003 [CrossRef Medline](#)
- Doubal FN, MacLulich AM, Ferguson KJ, et al. **Enlarged perivascular spaces on MRI are a feature of cerebral small vessel disease.** *Stroke* 2010;41:450–54 [CrossRef Medline](#)
- Granberg T, Moridi T, Brand JS, et al. **Enlarged perivascular spaces in multiple sclerosis on magnetic resonance imaging: a systematic review and meta-analysis.** *J Neurol* 2020;267:3199–3212 [CrossRef Medline](#)
- Joutel A, Faraci FM. **Cerebral small vessel disease: insights and opportunities from mouse models of collagen IV-related small-vessel disease and cerebral autosomal dominant arteriopathy with subcortical infarcts and leukoencephalopathy.** *Stroke* 2014;45:1215–21 [CrossRef Medline](#)
- Li Y, Zhu Z, Chen J, et al. **Dilated perivascular space in the mid-brain may reflect dopamine neuronal degeneration in Parkinson's disease.** *Front Aging Neurosci* 2020;12:161 [CrossRef Medline](#)
- Louveau A, Da Mesquita S, Kipnis J. **Lymphatics in neurological disorders: a neuro-lympho-vascular component of multiple sclerosis and Alzheimer's disease?** *Neuron* 2016;91:957–73 [CrossRef Medline](#)

22. Miyata M, Kakeda S, Iwata S, et al. **Enlarged perivascular spaces are associated with the disease activity in systemic lupus erythematosus.** *Sci Rep* 2017;7:12566 [CrossRef Medline](#)
23. Wardlaw JM, Smith C, Dichgans M. **Mechanisms of sporadic cerebral small vessel disease: insights from neuroimaging.** *Lancet Neurol* 2013;12:483–97 [CrossRef Medline](#)
24. Potter GM, Chappell FM, Morris Z, et al. **Cerebral perivascular spaces visible on magnetic resonance imaging: development of a qualitative rating scale and its observer reliability.** *Cerebrovasc Dis* 2015;39:224–31 [CrossRef Medline](#)
25. Mestre H, Kostrikov S, Mehta RI, et al. **Perivascular spaces, glymphatic dysfunction, and small vessel disease.** *Clin Sci (Lond)* 2017;131:2257–74 [CrossRef Medline](#)
26. Iliff JJ, Wang M, Liao Y, et al. **A paravascular pathway facilitates CSF flow through the brain parenchyma and the clearance of interstitial solutes, including amyloid beta.** *Sci Transl Med* 2012;4:147ra111 [CrossRef Medline](#)
27. Yang L, Kress BT, Weber HJ, et al. **Evaluating glymphatic pathway function utilizing clinically relevant intrathecal infusion of CSF tracer.** *J Transl Med* 2013;11:107 [CrossRef Medline](#)
28. Federico A, Di Donato I, Bianchi S, et al. **Hereditary cerebral small vessel diseases: a review.** *J Neurol Sci* 2012;322:25–30 [CrossRef Medline](#)
29. Yamamoto Y, Ihara M, Tham C, et al. **Neuropathological correlates of temporal pole white matter hyperintensities in CADASIL.** *Stroke* 2009;40:2004–11 [CrossRef Medline](#)
30. Yao M, Herve D, Jouvent E, et al. **Dilated perivascular spaces in small-vessel disease: a study in CADASIL.** *Cerebrovasc Dis* 2014;37:155–63 [CrossRef Medline](#)
31. Loos CM, Klarenbeek P, van Oostenbrugge RJ, et al. **Association between perivascular spaces and progression of white matter hyperintensities in lacunar stroke patients.** *PLoS One* 2015;10:e0137323 [CrossRef Medline](#)
32. Zhu YC, Tzourio C, Soumare A, et al. **Severity of dilated Virchow-Robin spaces is associated with age, blood pressure, and MRI markers of small vessel disease: a population-based study.** *Stroke* 2010;41:2483–90 [CrossRef Medline](#)
33. Potter GM, Doubal FN, Jackson CA, et al. **Enlarged perivascular spaces and cerebral small vessel disease.** *Int J Stroke* 2015;10:376–81 [CrossRef Medline](#)
34. Sorensen PS, Thomsen C, Gjerris F, et al. **Increased brain water content in pseudotumour cerebri measured by magnetic resonance imaging of brain water self-diffusion.** *Neurol Res* 1989;11:160–64 [CrossRef Medline](#)